

CONFERENCE.
AMORPHOUS, VITREOUS, AND POROUS SEMICONDUCTORS

Structural Transformations and Optical Properties of As₂S₃ Chalcogenide Glasses

I. V. Fekeshgazi*[^], K. V. Mai*, N. I. Matelesko**, V. M. Mitsa**, and E. I. Borkach**

* Lashkarev Institute of Semiconductor Physics, National Academy of Sciences of Ukraine, Kiev, 03028 Ukraine

[^] e-mail: fek_i@yahoo.com

** Uzhgorod National University, Uzhgorod, 88000 Ukraine

Submitted December 27, 2004; accepted for publication January 12, 2005

Abstract—The effects of melt temperature T_i and quenching rate V_i on the structure and optical properties of As₂S₃ glasses is studied. It is found that the glass band gap increases with T_i and V_i , whereas a decrease is observed in the glass density, refractive index (from 2.71 to 2.48), and two-photon absorption coefficient (from 0.37 to 0.15 cm/MW), which is accompanied by an increase in the optical-breakdown damage threshold.
© 2005 Pleiades Publishing, Inc.

1. INTRODUCTION

Chalcogenide arsenic trisulfide glasses are promising materials for fabricating various elements used in integrated optics, optoelectronics, and laser engineering [1–5]. At the same time, the rather low optical-breakdown damage of these glasses seriously restricts their wide application as power optics elements. It is known that the optical-breakdown damage of a material is controlled by its optical quality (the degree of homogeneity and the existence or absence of mechanical stresses and impurities), on which linear and nonlinear absorption and scattering losses depend. In turn, the optical quality of glasses depends on their synthesis conditions, under which various structural-topological groups are formed in the bulk. An analysis of results regarding the effect of structural-topological transformations on the refractive index (n), linear (α) and two-photon (β) absorption constants, and Raman scattering (RS) spectra, as well as on the dynamic and optical-breakdown damage of arsenic trisulfide (As₂S₃) glasses, is carried out.

2. SAMPLE PREPARATION AND METHODS OF STUDY

The most commonly used method for the fabrication of bulk glasses is rapid quenching of a material melt. The studies were carried out using samples synthesized from the elemental components As and S (ultra-pure grade, 99.99999%) at three melt temperatures (T) and three quenching rates (V). The temperature $T_1 = 870$ K is the lowest temperature at which an arsenic-sulfur interaction corresponds to a real time scale (~150 h), $T_2 = 1120$ K is the temperature at which arsenic sulfides are typically synthesized, and $T_3 = 1370$ K is the highest temperature at which As₂S₃ molecules retain their structure before being dissociated into elementary components.

The rate $V_1 = 10^{-2}$ K/s corresponds to cooling of the melt in a technological furnace, $V_2 = 1.5$ K/s is the cell cooling rate in air at room temperature and is the optimum rate for synthesizing arsenic sulfide, and the rate $V_3 = 150$ K/s corresponds to cell cooling in ice water (0°C). The glass microstructure was studied using an EMV-100B transmission electron microscope (TEM) at an accelerating voltage of 100 kV [6]. Samples 20–50 nm thick were prepared using a piezoelectric microtome with a tray for distilled water. Freshly cleaved fragments were caught on a copper grid and, immediately after drying, placed into the microscope column.

The bulk structure of the glasses was analyzed using the conventional criteria of microdispersity and microinhomogeneity degrees, which were determined as the ratio of the number of distinctly contoured boundaries to the number of pseudo-grains per 0.1- μ m-long segment.

The linear-loss and two-photon absorption coefficients were determined using experimentally measured dependences of the intensity I of transmitted light on the intensity I_0 of light incident on the sample. These dependences were sublinear (Fig. 1, curve I) and adequately described by the formula (see [7, 8])

$$I = I_0 \frac{(1 - R_0)^2 \exp(-\alpha d)}{1 + \beta I_0 \alpha^{-1} (1 - R_0) [1 - \exp(-\alpha d)]},$$

where R_0 is the light reflectance from the surface of a sample of thickness d and α and β are the linear-loss and two-photon absorption coefficients, respectively.

The inverse transmittance

$$I_0/I = \frac{1 + \beta I_0 \alpha^{-1} (1 - R_0) [1 - \exp(-\alpha d)]}{(1 - R_0)^2 \exp(-\alpha d)}$$

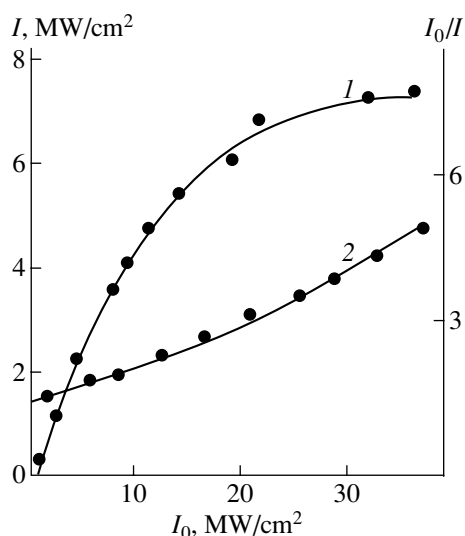


Fig. 1. Dependences of the transmitted light intensity I (1) and the ratio I_0/I (2) on the ruby laser light intensity I_0 .

is directly proportional to I_0 (Fig. 1, curve 2), which indicates the dominant contribution of two-photon transitions to the nonlinear light absorption.

The linear-loss α and two-photon absorption β coefficients calculated from the dependences shown in Fig. 1 are listed in the table.

The optical-breakdown threshold I_b was determined as the lowest density of laser radiation at which a bright flash was observed at the sample surface and, as a consequence, the intensity of the transmitted ruby laser 20-ns pulse abruptly decreased (at the half-maximum of the Gaussian time distribution).

3. RESULTS AND DISCUSSION

Various structural-topological elements were formed by varying the glass synthesis conditions (T_i and V_i). It was found that variation in T_i and V_i within the indicated ranges yielded a basic set of possible structural groups, which could be divided into two main

types: a homogeneous *A* set mostly containing the bipyramidal structural units $\text{AsS}_{3/2}$, which are inherent in glasses with a microdisperse structure of various degrees of cohesion and a continuous structural network, and a *B* set containing the heteroatomic pseudo-molecular units $\text{As}_2\text{S}_{4/2}$, As_3S_3 , As_2S_5 and homogeneous sulfur aggregates S_8 . These results are also confirmed by a comparative analysis of the Raman scattering (RS) spectra of arsenic trisulfide glasses in the stretching vibration range [9, 10]. Types *A* and *B* appear at the lowest and highest values of T_i and V_i , respectively. As T_i and V_i increased, the glass band gap (E_g) increased, the density ρ decreased, the refractive index and two-photon absorption coefficient decreased (from $n = 2.71$ to 2.58 cm/MW and from $\beta = 0.37$ to 0.15 cm/MW, respectively) (Fig. 2), and there was an accompanying corresponding increase in the optical-breakdown damage threshold I_b (see table).

Electron microscopy study of the glass bulk showed that operating conditions T_1 and V_1 yield a homogeneous matrix with uniformly distributed microcrystalline As_2S_3 inclusions 4–10 nm in size. At T_1 and V_2 , as well as at T_1 and V_3 , there existed cohered microdisperse pseudograins 1–2 nm in size and spherical microinclusions 5–10 nm in diameter, respectively. Under conditions T_2 and V_1 , as well as T_2 and V_2 , the glass structure was similar to that obtained at T_1 and V_2 . Conditions T_3 and V_1 yielded a rather homogeneous microstructure consisting of cohered microdisperse drop-shaped pseudograins smaller than 50 nm in diameter. At T_3 and V_2 , a rather homogeneous composition of heterogeneous pseudograins 5–10 nm in size was observed. At T_3 and V_3 , there was a relatively uniform distribution of 30- to 50-nm spherical microinclusions in a microdisperse matrix.

The spectral dependences of the linear absorption coefficient near the intrinsic absorption edge are complicated. These dependences, in combination with nonlinear optical losses, control the glass optical-breakdown damage to laser beam fluxes.

A comparative analysis of the RS spectra of the arsenic trisulfide glasses in the stretching vibration

Physical parameters of vitreous As_2S_3

T_i , K	V_i , K/s	ρ , g/cm ³	E_g , eV	n (633 nm)	α , cm ⁻¹	β , cm/MW	I_b , MW/cm ²
$T_1 = 870$	$V_1 = 10^{-2}$	3.201	2.12	2.712	2.16	0.37	30
	$V_2 = 1.5$	3.195	2.15	2.69	1.17	0.16	45
	$V_3 = 150$	3.192	2.21	2.664	2.22	0.15	55
$T_2 = 1120$	$V_1 = 10^{-2}$	3.193	2.18	2.705	1.96	0.4	30
	$V_2 = 1.5$	3.190	2.22	2.65	2.53	0.25	36–40
	$V_3 = 150$	3.186	2.26	2.602	1.305	0.18	30–40
$T_3 = 1370$	$V_1 = 10^{-2}$	3.192	2.22	2.602	1.90	0.24	30
	$V_2 = 1.5$	3.184	2.30	2.59	1.855	0.17	36–40
	$V_3 = 150$	3.176	2.38	2.580	1.73	0.15	50–60

range showed that the concentration of $As_2S_{4/2}$, $As_{3/3}$, S_8 , and S_n structural units in the glass matrix structure increased with T_i and V_i [9]. In this case, the degree of structure rarefaction increased (the density decreased), and the ultrasound velocity in the As_2S_3 glass decreased; hence, the glass dynamic stability, expressed in terms of elastic moduli, decreased.

The results of this study confirm that low-frequency RS spectroscopy in the “boson peak” region, combined with ultrasonic studies, is an efficient method for determining the degree of structural correlation in glasses when various approximations of their structure are applied [10]. The resolution of low-frequency RS spectroscopy is better than that of neutron diffraction in the same spectral region.

As the synthesis conditions of As_2S_3 glasses were varied, i.e., the melt temperature and quenching rate were increased (except in the case of conditions T_1 and V_2), a low-frequency shift of the “boson peak” from 26 cm^{-1} (T_1 and V_1) to 20 cm^{-1} (T_3 and V_3) was observed. This was accompanied by an increase in the structural correlation radius (R) and length (L), respectively, in the homogeneous and chain approximations of the glass structure. The relation $L/R \approx 2$ is valid in all cases.

Furthermore, it was found that the low-frequency peak shifts to higher frequencies, from 19 cm^{-1} ($z = 2.1$) to 26 cm^{-1} ($z = 2.4$), as the average coordination number $z = 3y + 2(1 - y)$ increased in the binary As_yS_{1-y} glasses. This increase was accompanied by a decrease in the chain length L from 1.5 to 1.4 nm. The smallest value of L , $L = 1.42\text{ nm}$, at $z = 2.4$ corresponded to a dynamic stability maximum. The changes in the coordination number (from $z = 2.1$ to 2.4) and the corresponding increase in the elastic moduli of the As_yS_{1-y} glasses were consistent with the cluster topology (CT) concept on an increase in the dynamic stability of the glass matrix structure due to the strengthening of the inter-chain interaction and merging of one-dimensional clusters into layered-chain clusters near the composition $As_{40}S_{60}$ ($z = 2.4$) ($1D \rightarrow 2D$ transition). A change from the $As_{40}S_{60}$ composition to arsenic-enriched compositions ($As_{42}S_{58}$) resulted in an increase in the low-frequency vibration intensity and growth of the chain clusters. As L increased, the glass dynamic stability decreased at $z > 2.4$, and the increase in the elastic moduli deviated from that predicted by the CT concept (according to the law $(z - 2.4)^{3/2}$). The detected rarefaction of the matrix structure of the As_yS_{1-y} glasses at $z > 2.4$ was accompanied by formation of the new structural units $As_2S_{4/2}$ and $As_{3/3}$.

A decrease in the two-photon absorption coefficient with T_i or V_i is caused by an increase in the band gap [11, 12]. The optical-breakdown damage estimated in the adiabatic approximation differed from the experimental data by almost three orders of magnitude. At the

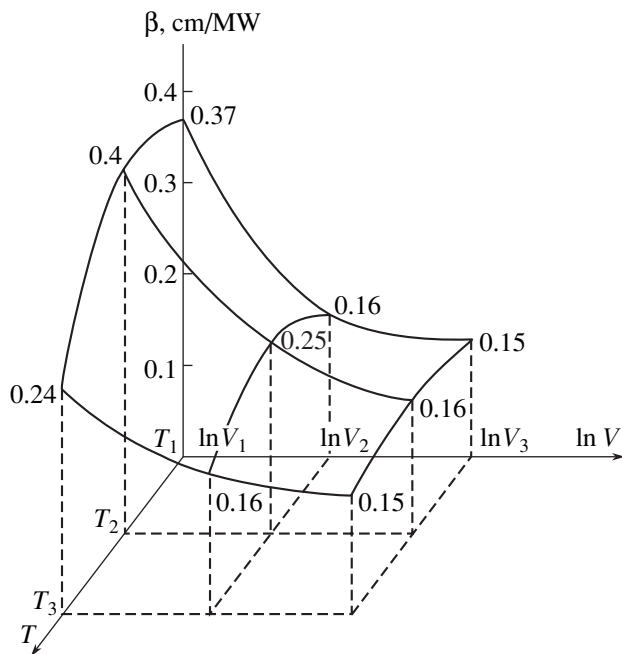


Fig. 2. Dependences of the two-photon absorption constant β on the melt temperature T_i and quenching rate V_i of the As_2S_3 glasses.

same time, according to the theory, the optical-breakdown damage threshold increases, since the linear and nonlinear loss coefficients decrease, whereas the band gap widens.

4. CONCLUSIONS

The systematic features of glass microstructure formation depending on melt temperature and quenching rate have been established using electron microscopy. It is shown that, optically, most homogeneous glasses are obtained under T_1 and V_2 , T_2 and V_1 , and T_2 and V_2 conditions.

The glass band gap increases with T_i and V_i , while a decrease is observed in the glass density, refractive index (from 2.71 to 2.48), and two-photon absorption coefficient (from 0.37 to 0.15 cm/MW), which is accompanied by an increase in the optical-breakdown damage threshold.

ACKNOWLEDGMENTS

This study was supported by the State Foundation for Basic Research of the Ministry of Education and Science of Ukraine, project no. F 7/273-2001.

REFERENCES

1. Z. U. Borisova, *Chalcogenide Semiconducting Glasses* (Leningr. Gos. Univ., Leningrad, 1983) [in Russian].
2. A. Feltz, *Amorphe und Glasartige Anorganische Festkörper* (Akademie, Berlin, 1983; Mir, Moscow, 1986).

3. S. V. Svechnikov, V. V. Khiminets, and N. I. Dovgosheĭ, *Complex Noncrystalline Chalcogenides and Chalcohalides and Their Application in Optoelectronics* (Naukova Dumka, Kiev, 1992) [in Russian].
4. G. Z. Vinogradova, *Glass-Formation and Phase Equilibria in Chalcogenide Systems* (Nauka, Moscow, 1984) [in Russian].
5. M. Bertolotti, V. Chumash, E. Fazio, *et al.*, *J. Appl. Phys.* **74**, 3024 (1993).
6. N. Mateleshko and E. Borkach, *Semicond. Phys. Quantum Electron. Optoelectron.* **7**, 171 (2004).
7. I. V. Fekeshgazi, K. V. May, V. M. Mitsa, and V. V. Roman, *Proc. SPIE* **2648**, 257 (1995).
8. V. V. Grabovskii, K. V. May, V. I. Prokhorenko, *et al.*, *J. Appl. Spectrosc.* **63**, 586 (1996).
9. R. Holomb and V. Mitsa, *Solid State Commun.* **129**, 655 (2004).
10. R. Golomb, N. Veresh, M. Koosh, and M. Gomeš, in *Proceedings of 4th International Conference on Amorphous and Microcrystalline Semiconductors* (St. Petersburg, 2004), p. 220.
11. I. Fekeshgazi, K. May, V. Mitsa, *et al.*, *Proc. SPIE* **2968**, 256 (1997).
12. I. V. Fekeshgazi, K. V. Maĭ, A. P. Klimenko, *et al.*, in *Proceedings of 4th International Conference on Amorphous and Microcrystalline Semiconductors* (St. Petersburg, 2004), p. 152.

Translated by A. Kazantsev